

Identification of an Additional Interaction Domain in Transmembrane Domains 11 and 12 That Supports Oligomer Formation in the Human Serotonin Transporter*

Received for publication, June 10, 2003, and in revised form, November 14, 2003
Published, JBC Papers in Press, December 5, 2003, DOI 10.1074/jbc.M306092200

Herwig Just[‡], Harald H. Sitte[‡], Johannes A. Schmid[§], Michael Freissmuth[‡],
and Oliver Kudlacek[‡]

From the [‡]Institute of Pharmacology, University of Vienna Medical School, Währinger Strasse 13A, A-1090 Vienna, Austria and the [§]Department of Vascular Biology and Thrombosis Research, University of Vienna Medical School, Brunnerstrasse 59, A-1235 Vienna, Austria

Na⁺/Cl⁻-dependent neurotransmitter transporters form constitutive oligomers. The topological arrangement is not known, but a leucine heptad repeat in transmembrane domain (TM) 2 and a glycoprotein-like motif in TM6 have been proposed to stabilize the oligomer. To determine the topology, we generated versions of the human serotonin transporter (hSERT) that carried cyan or yellow fluorescent proteins at their amino and/or carboxyl terminus. Appropriate pairs were coexpressed to measure fluorescence resonance energy transfer (FRET). Donor photobleaching FRET microscopy was employed to deduce the following arrangement: within the monomer, the amino and carboxyl termini are in close vicinity. In addition, in the oligomer, the carboxyl termini are closer to each other than the amino termini. Hence, a separate interaction domain (*i.e.* distinct from TM2 and TM6) must reside in the carboxyl-terminal half of hSERT. This was confirmed by expressing the amino- and carboxyl-terminal halves of hSERT. These were retained intracellularly; they also retained the coexpressed full-length transporter by forming export-deficient oligomers and, when cotransfected in all possible combinations, supported FRET. Hence, both the carboxyl and amino termini contain elements that drive oligomerization. By employing fragments comprising two neighboring TM helices, we unequivocally identified TM11/12 as a new contact site by donor photobleaching FRET and β -lactamase protein fragment complementation assay. TM1/2 was also found to self-associate. Thus, oligomerization of hSERT involves at least two discontinuous interfaces. The currently identified interaction sites drive homophilic interactions. This is consistent with assembly of SERT oligomers in an array-like structure containing multimers of dimers.

Under physiological conditions, the serotonin transporter (SERT)¹ mediates the selective re-uptake of 5-hydroxy-

tryptamine (5-HT; serotonin) that has been released into the synaptic cleft by neurons. SERT is of clinical relevance because it is the target of antidepressants. It is also the site of action for drugs of abuse, *viz.* ecstasy (methylenedioxymetamphetamine) and its congeners; these compounds release serotonin because they induce reverse transport (1).

The hydrophobic core of SERT consists of 12 transmembrane domains (TMs); this structural feature is shared by all neurotransmitter transporters and by many other transporters (*e.g.* P-glycoprotein-like efflux pumps) and membrane proteins (*e.g.* mammalian isoforms of membrane-bound adenylyl cyclase). Several Na⁺/Cl⁻-dependent neurotransmitter transporters have been shown to form constitutive oligomers in the plasma membrane (2–8). Although the precise biological role of oligomerization remains enigmatic, there are many arguments that support the conjecture that oligomer formation is a prerequisite for export from the endoplasmic reticulum (ER) (reviewed in Ref. 9). The topological arrangements of the 12 TM helices is not known; in the recently solved structure of two distantly related bacterial transporters, the first six TM helices and the carboxyl-terminal six helices are arranged in two pseudosymmetrical lobes around the central pore (10, 11). The connecting loops that connect the TM helices are substantially shorter in human SERT (hSERT) than in the bacterial transporters. Thus, it is likely that the topology of the hydrophobic core differs substantially in hSERT. However, it is reasonable to predict that the 12 TM helices are arranged in a ring-like structure around a central substrate-binding cavity. The ring-like structure ought to allow for a number of contacts between individual transporter monomers. In a dimeric arrangement, a self-limiting structure is achieved by a symmetric interface, *i.e.* via homophilic interactions. However, in all other instances (*e.g.* trimers or tetramers), there must be more than one interface, and these contact sites must represent, at least in part, interactions between distinct segments, *i.e.* heterophilic interactions (12). In this work, we have examined these predictions by generating several tagged versions of hSERT. This allowed us to confirm the close proximity of amino and carboxyl termini. In addition, we identified at least two discontinuous contact sites that support homophilic interactions. Based on these observations, we propose that SERT may have the propensity to form an array-like structure in the membrane.

EXPERIMENTAL PROCEDURES

Construction of Fluorescently Tagged hSERT and hSERT Fragments—We used plasmids pECFP-N1/pEYFP-N1 and pECFP-C1/

(1R,2S,3S,5S)-3-(4-iodophenyl)-8-[³H]methyl-8-azabicyclo[3.2.1]octane-2-carboxylic acid, methyl ester; hD2, human dopamine D₂ receptor.

* This work was supported by Austrian Science Foundation Grants P15034 (to M. F.) and P14509 (to H. H. S.) and by a grant (“Epileptosome”) from European Union Framework Program 5. The costs of publication of this article were defrayed in part by the payment of page charges. This article must therefore be hereby marked “advertisement” in accordance with 18 U.S.C. Section 1734 solely to indicate this fact.

† To whom correspondence should be addressed. Tel.: 43-1-4277-64171; Fax: 43-1-4277-9641; E-mail: michael.freissmuth@univie.ac.at.

¹ The abbreviations used are: SERT, serotonin transporter; hSERT, human SERT; 5-HT, 5-hydroxytryptamine; TM, transmembrane domain; ER, endoplasmic reticulum; YFP and CFP, yellow and cyan fluorescent protein, respectively; FRET, fluorescence resonance energy transfer; DRAP, donor recovery after acceptor photobleaching; [³H] β -CIT,

pEYFP-C1 (Clontech) to drive expression of the fluorescent full-length transporter and fragments thereof in mammalian cells. YFP/CFP-hSERT (hSERT Met¹-Val⁶³⁰ carrying YFP or CFP at its amino terminus) has been described previously (3). PCR² was employed to generate the following additional constructs (see also Fig. 1A for an overview): hSERT-YFP/CFP (hSERT Met¹-Val⁶³⁰ fused to YFP or CFP at its carboxyl terminus) and CFP-hSERT-YFP (hSERT Met¹-Val⁶³⁰ carrying CFP at its amino terminus and YFP at its carboxyl terminus). Severing the double-tagged hSERT in the middle yielded two constructs: YFP/CFP-hSERT-N-term (hSERT Met¹-Asn³⁵⁶ with amino-terminal YFP or CFP) comprising TM1–6 and hSERT-C-term-YFP/CFP (hSERT Cys³⁵⁷-Val⁶³⁰ with carboxyl-terminal YFP or CFP) comprising TM7–12. YFP-labeled fragments were created that comprised two neighboring TM helices: YFP-hSERT-TM1/2 (hSERT Met¹-Ile¹⁵⁰), YFP-hSERT-TM3/4 (hSERT Trp¹⁵¹-Gly²⁷⁸), YFP-hSERT-TM5/6 (hSERT Lys²⁷⁵-Asn³⁵⁷), YFP-hSERT-TM7/8 (hSERT Cys³⁵⁷-Leu⁴⁵¹), YFP-hSERT-TM 9/10 (hSERT Asp⁴⁵²-Arg⁵²³), and hSERT-TM11/12-YFP (hSERT Lys⁵²⁶-Val⁶³⁰). The integrity of each engineered construct was verified by fluorescent sequencing.

Cell Transfection, Uptake Experiments, and Fluorescence Resonance Energy Transfer (FRET) Microscopy—The conditions for cell culture and the uptake experiments have been described in detail elsewhere (3). The calcium phosphate method was used for transient transfection. Donor photobleaching FRET microscopy was performed as described previously (10). To measure donor recovery after acceptor photobleaching (DRAP), we acquired a donor (CFP) image before (I_0) and after (I_a) photobleaching using the YFP setting for 90 s (excitation = 500 nm, dichroic mirror = 525 nm, and emission = 535 nm). DRAP was quantified by FRET efficiency (E) as described by Miyawaki and Tsien (14) according to the following equation: $E = (I_a - I_0)/I_a$.

Membrane Preparation and Radioligand Binding—Cells were detached mechanically, lysed by a freeze-thaw cycle, and homogenized in buffer containing 20 mM Tris-HCl (pH 8), 1 mM EDTA, 2 mM MgCl₂, and 300 mM sucrose. Membranes were sedimented by centrifugation at 50,000 × g for 20 min (10). Binding of [³H]β-CIT (specific activity of ~50 Ci/mmol; Tocris, Bristol, United Kingdom) was determined in a final volume of 40 μl containing 20 mM Hepes-NaOH (pH 7.4), 2 mM MgCl₂, 1 mM EDTA, cell membranes (10 μg for full-length SERT constructs and 50 μg for the severed transporters), and concentrations of [³H]β-CIT ranging from 0.25 to 10 nM. The reaction was carried out for 60 min at room temperature. Nonspecific binding was determined in the presence of 3 μM paroxetine and was <10% of total binding in the K_D range for full-length constructs. Bound and free radioligands were separated by filtration over glass-fiber filters.

β-Lactamase Protein Fragment Complementation Assay—For the β-lactamase protein fragment complementation assay, we used plasmids pcDNA3.1-Zeo+/F[II]m182T and pcDNA3.1-Zeo+/F[III] to drive the expression of proteins fused to β-lactamase fragments F[II] and F[III] (15). Constructs of hSERT that comprised two neighboring TM helices were generated by PCR²: F[II]-TM1/2 and F[III]-TM1/2 (hSERT Gly⁸³-Gly¹⁴⁶), F[II]-TM5/6 and F[III]-TM5/6 (hSERT Val²⁷⁴-Asn³⁵⁶), and F[II]- and F[III]-TM11/12 (hSERT Phe⁵³⁶-Thr⁶⁰⁰). Cells were transfected with the indicated combinations of plasmids using LipofectAMINE. After 24–48 h, cells were detached mechanically, lysed by a freeze-thaw cycle, and homogenized in phosphate-buffered saline. Membranes were sedimented by centrifugation at 50,000 × g for 20 min, and pellets were resuspended in phosphate-buffered saline. The membrane suspension (20-μl aliquot) was incubated in the presence of 100 μM nitrocefin in phosphate-buffered saline in a total volume of 200 μl for 45 min at 37 °C. Absorption at 492 nm was measured using an automated plate reader.

RESULTS

Characterization of Tagged hSERT and Half-molecules—The topology of neurotransmitter transporters is not known; and in particular, it is not clear how individual monomers assemble into the oligomeric structure that resides in the plasma membrane. Previous experiments showed that, when tagged with fluorescent proteins, the amino termini of hSERT are close enough to support FRET. Resonance energy transfer is exquisitely sensitive to variation in distance, with energy transfer declining with the sixth power of distance. We therefore generated additional fusion proteins comprising hSERT

and the spectral variants of the green fluorescent protein, CFP and YFP. Fig. 1A shows a schematic rendering of the hSERT constructs that were employed.

We ruled out that the position of the fluorescent protein tag interfered with hSERT function: the K_m for inward transport of the substrate was comparable regardless of whether the fluorescent protein was attached to the amino terminus (CFP-hSERT; $K_m = 1.5 \pm 0.7 \mu\text{M}$, $n = 3$) (Fig. 1B, *closed squares*), the carboxyl terminus (hSERT-CFP; $K_m = 2.5 \pm 0.8 \mu\text{M}$, $n = 3$) (*inverted closed triangles*), or both (CFP-hSERT-YFP; $K_m = 1.5 \pm 0.6 \mu\text{M}$; $n = 3$) (*closed circles*). The K_m determined in parallel for the transiently expressed untagged wild-type hSERT protein (Fig. 1B, *open triangles*) was $2.6 \pm 0.6 \mu\text{M}$ ($n = 3$). Differences in the maximum velocity of uptake (V_{max}) can be accounted for by variations in expression levels. This can be gauged from the saturation experiment depicted in Fig. 1C, where differences in B_{max} levels essentially reflect the variability in the velocity of uptake (Fig. 1, compare B and C). The affinity of the inhibitor β-CIT for the tagged full-length transporters was virtually identical ($K_D = 1.2 \pm 0.2$, 1.5 ± 0.3 , 2.1 ± 1.7 , and 1.3 ± 0.2 nM for CFP-hSERT-YFP, CFP-hSERT, hSERT-CFP, and hSERT, respectively; $n = 3$). In contrast, if SERT was severed, the resulting half-molecules failed to transport substrate and to bind the inhibitor regardless of whether the amino-terminal (Fig. 1B, *open circles*) and carboxyl-terminal (*open squares*) fragments were expressed alone or in combination (Fig. 1, B and C, *closed diamonds*).

Segments of the amino and carboxyl termini are thought to support the interaction of hSERT (16) and related transporters such as the γ-aminobutyric acid (17–19), dopamine (20), and norepinephrine (21) transporters with proteins that are important for insertion into and retention at the plasma membrane. We therefore verified that the presence of the fluorescent tag did not interfere with insertion of SERT into the plasma membrane. As shown in Fig. 1D, provided that hSERT was expressed as a full-length protein, it was efficiently inserted into the plasma membrane regardless of whether the fluorescent protein was fused to the amino terminus, the carboxyl terminus, or both. This was also seen upon expression in differentiated PC12 cells, where all full-length versions of hSERT were efficiently transported to the extending neurite (data not shown). In contrast, the severed half-transporters that comprised only the amino- or carboxyl-terminal six TM segments (CFP-hSERT-N-term and hSERT-C-term-CFP) were invariably retained within the cell (Fig. 1D). This intracellular retention was not overcome by coexpression of the half-molecules (data not shown). Finally, we also verified that the presence of a YFP moiety did not affect 5-HT transport by hSERT ($K_m = 0.9 \pm 0.2 \mu\text{M}$ for YFP-hSERT, and $K_m = 1.1 \pm 0.3 \mu\text{M}$ for hSERT-YFP), inhibitor binding, and subcellular localization (data not shown in Fig. 1).

FRET Microscopy with Amino- and Carboxyl-terminally Tagged Versions of hSERT—There are several ways to assess resonance energy transfer. Previously, we employed two methods, *viz.* ratio imaging, and determination of fluorescence decay after donor photobleaching, to demonstrate that YFP-hSERT and CFP-hSERT formed a constitutive oligomer (2). In the present study, we relied primarily on measuring the decay lifetimes after donor photobleaching because this allows for a statistical comparison provided that the number of measurements is large enough (and provided that the measurements are done in parallel to account for inherent variations in lamp intensity). The serpentine diagram depicted in Fig. 1A is misleading, for it suggests a maximum distance between the amino and carboxyl termini. However, the transporter has to provide for a pore, *i.e.* a hydrophilic channel, which allows for TM

² Primer sequences are available upon request.

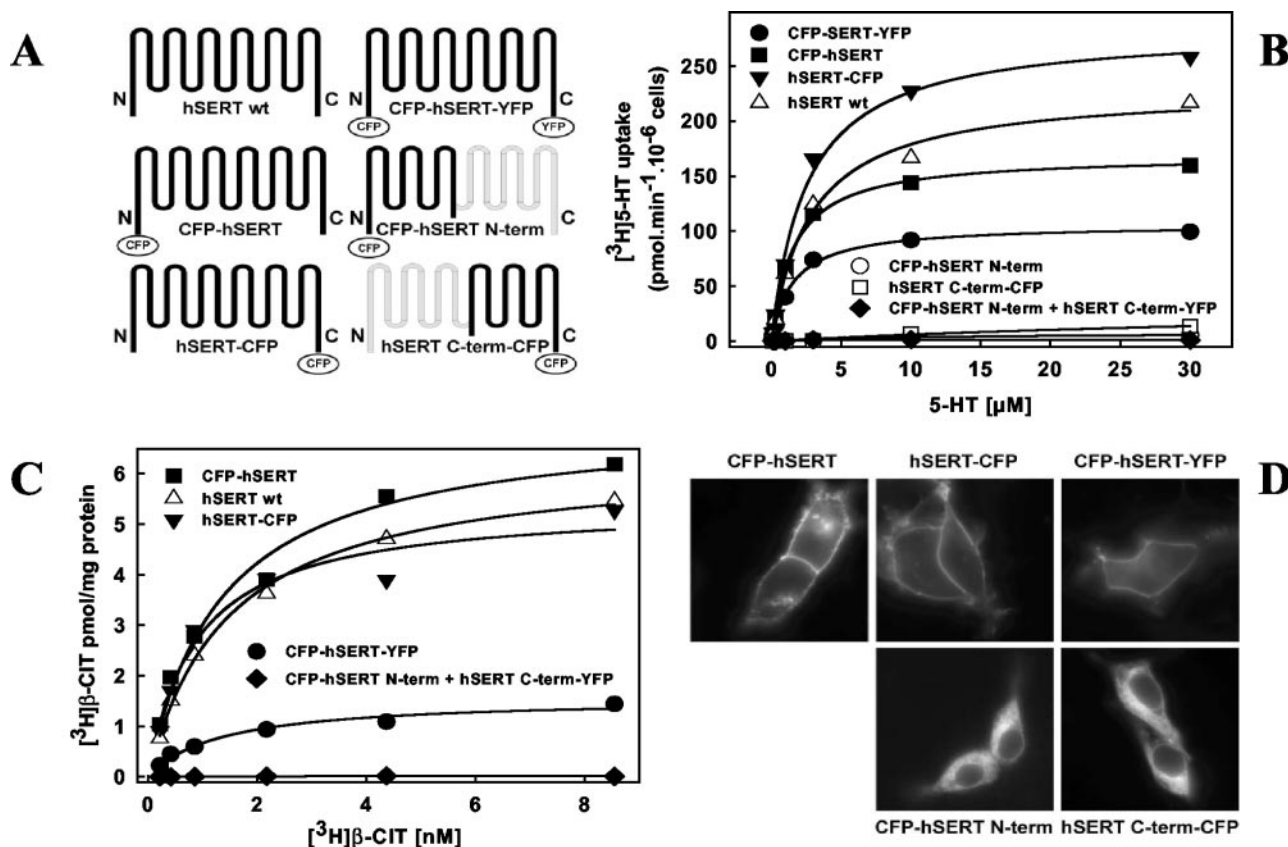


FIG. 1. Schematic rendering (A), functional characterization (B and C), and subcellular localization (D) of fluorescently labeled hSERT constructs. A, full-length hSERT was tagged with YFP or CFP at its amino terminus (YFP/CFP-hSERT), at its carboxyl terminus (hSERT-YFP/CFP), or at both ends (CFP-hSERT-YFP). The molecule was severed to generate tagged halves comprising TM1–6 (YFP/CFP-hSERT-N-term) or TM7–12 (hSERT-C-term-YFP/CFP). Finally, YFP-labeled fragments were generated that comprised two neighboring TM helices (YFP-hSERT-TM1/2, -TM3/4, -TM5/6, -TM7/8, and -TM9/10 and hSERT-TM11/12-YFP) (data not shown). B and C, HEK293 cells were transfected with plasmids encoding different hSERT constructs. Closed squares, CFP-hSERT; inverted closed triangles, hSERT-CFP; closed circles, CFP-hSERT-YFP; open triangles, wild-type (wt) hSERT; open circles, CFP-hSERT-N-term; open squares, hSERT-C-term-CFP; closed diamonds, CFP-hSERT-N-term + hSERT-C-term-YFP. Uptake of $[^3\text{H}]\text{5-HT}$ (B) by transiently transfected cells (10^5 cells/well) was determined in 0.1 ml of HEPES-buffered Krebs solution containing the indicated concentrations of $[^3\text{H}]\text{5-HT}$ (specific activity of 15 cpm/fmol to 50 cpm/pmol). The incubation lasted for 1 min at 25 °C. Binding of $[^3\text{H}]\beta\text{-CIT}$ (C) to membranes (50 μg /assay) prepared from the same transiently transfected cell batch used in B was determined as described under “Experimental Procedures.” D, HEK293 cells were transfected with plasmids encoding CFP-hSERT, hSERT-CFP, CFP-hSERT-YFP, CFP-hSERT-N-term, and hSERT-C-term-CFP. Images (magnification $\times 63$) were captured using the CFP filter set.

permeation of the substrate and the cotransported ions. Thus, it is more plausible that the helices arrange in a ring-like structure in which amino and carboxyl termini are in close vicinity. Accordingly, the decay of fluorescence was substantially slower in the double-tagged CFP-hSERT-YFP than in the coexpressed pair CFP-hSERT/hSERT-YFP (Fig. 2, A–C). The addition of substrates or inhibitors did not result in any appreciable change of energy transfer (data not shown).

Donor photobleaching FRET microscopy relies on the fact that energy transfer to the acceptor protects the donor against bleaching. For a given pair of FRET fluorophores (e.g. CFP and YFP), the protection (and hence, the increase in the decay lifetime) depends on the distance between acceptor and donor and on their relative orientation. Based on the data shown in Fig. 2C, the carboxyl and amino termini are more closely associated than the amino termini. However, it is obviously not possible to differentiate between intra- and intermolecular energy transfer in CFP-hSERT-YFP. To assess the contribution of intermolecular energy transfer, we determined fluorescence decay lifetimes for the combination YFP-hSERT and hSERT-CFP and, as an internal control, the reverse pair, CFP-hSERT and hSERT-YFP. As shown in Fig. 2C, the lifetimes for these two pairs were virtually identical and shorter than for the double-tagged CFP-hSERT-YFP. This indicates that the intramolecular distance between amino and carboxyl termini is

smaller than the intermolecular distance. On the other hand, the lifetimes obtained for the pairs of amino- and carboxyl-terminally tagged transporters (e.g. YFP-hSERT and hSERT-CFP) were longer than that obtained for the combination in which both donor and acceptor resided on the amino terminus (i.e. YFP-hSERT and CFP-hSERT). Finally, we tested a pair of carboxyl-terminally tagged transporters. The lifetime determined for this combination again exceeded that of the amino-terminally tagged transporters.

FRET is exquisitely sensitive to the distance of the fluorophore, i.e. it declines with the sixth power of the distance; in addition, resonance energy transfer is affected by the orientation of the fluorophores (22, 23). The observations indicated that the intermolecular distance between the carboxyl termini was smaller than that of the amino termini. Alternatively, and less likely, the relative orientation of the dipoles may have been more favorable if the two fluorophores were attached to the carboxyl termini rather than to the amino termini or to each an amino and a carboxyl terminus. However, the interpretation of the differences in lifetimes relies on the assumption that the amount of acceptor fluorophore is not limiting in the vicinity of the donor. In transient transfection, expression levels vary widely from cell to cell. The data displayed in Fig. 2C were obtained by selecting for cells that displayed bright acceptor fluorescence. In addition, we also carried out a separate series

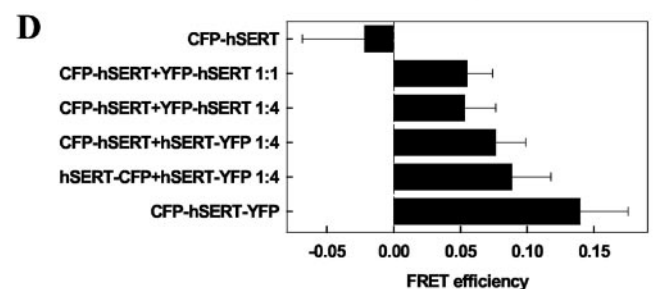
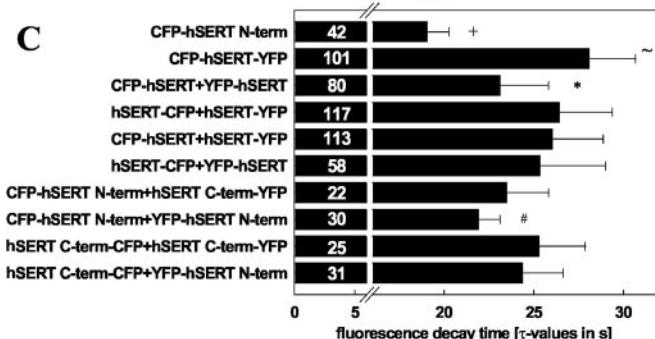
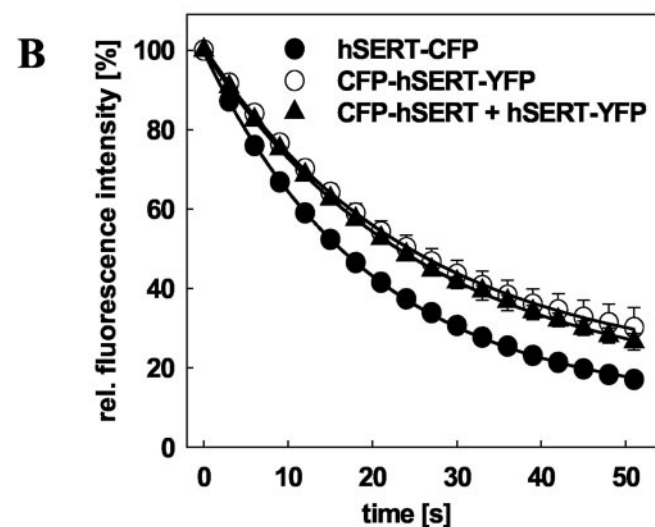
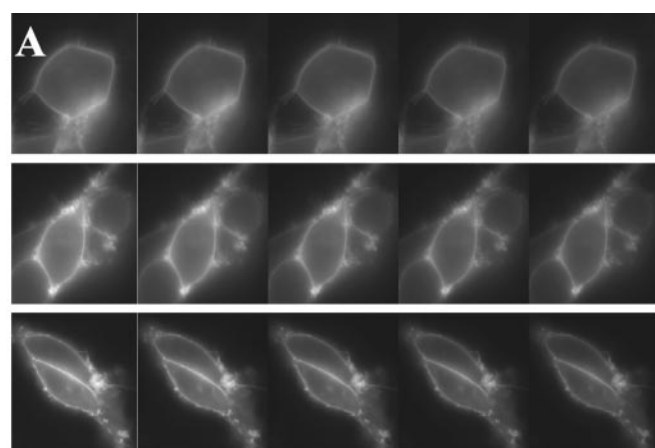


FIG. 2. Donor photobleaching and DRAP FRET microscopy of full-length hSERT constructs. The indicated combinations of fluorescent protein-labeled full-length hSERT constructs were coexpressed in HEK293 cells ($1 \mu\text{g}$ of donor plasmid and $2 \mu\text{g}$ of acceptor plasmid); donor photobleaching (A–C) and DRAP (D) FRET microscopy was performed 24–48 h after transfection. A–C, photobleaching of the donor (CFP) was achieved by illuminating the cell at the center of the visual field with a mercury arc lamp (Zeiss HBO, 100-watt intensity) for 60 s. Images were captured every 3 s, digitized, and stored. A, representative images (3-s intervals) illustrate the decrease in the donor fluorescence

of experiments in which the ratio of plasmid encoding the donor and that encoding the acceptor was varied between 1:1 and 1:4 (using the combinations CFP-hSERT + YFP-hSERT, CFP-hSERT + hSERT-YFP, and hSERT-CFP + hSERT-YFP), and resonance energy transfer was determined by DRAP. There was not any appreciable difference in resonance energy transfer if the amount of plasmid encoding the acceptor was increased 4-fold (shown in Fig. 2D for the combination CFP-hSERT + YFP-hSERT). The DRAP experiment also confirmed that FRET efficiency was higher with the carboxyl-terminally tagged combination (hSERT-CFP + hSERT-YFP) than if the fluorophores were attached to the amino termini (CFP-hSERT + hSERT-YFP) (Fig. 2D). The double-tagged transporter (CFP-hSERT-YFP) showed the highest FRET efficiency ($p < 0.001$).

Oligomer Formation by Half-molecules—The intracellular carboxyl terminus of hSERT comprises 35 amino acids, which may provide for a flexible tether of the fluorescent protein tag. Hence, the short intermolecular distance between the carboxyl termini does not necessarily indicate that the carboxyl-terminal TM segments support any association in the oligomer. We therefore engineered constructs that allowed for the expression of half-molecules to test if the carboxyl-terminal half of hSERT supports self-association. These half-transporters were retained within the cell (Fig. 1D). Nevertheless, donor photobleaching experiments showed that they were capable of self-association. This was true for the combination CFP-hSERT-N-term + YFP-hSERT-N-term as well as for hSERT-C-term-CFP + hSERT-C-term-YFP (Fig. 2C). In cells expressing the donor alone (CFP-hSERT-N-term), the lifetime of fluorescence decay was 19.1 ± 1.2 s ($n = 42$). Coexpression of CFP- and YFP-labeled amino-terminal halves increased it to 21.9 ± 1.2 s ($n = 30$) (CFP-hSERT-N-term + YFP-hSERT-N-term) and to 25.3 ± 2.6 s ($n = 25$) (hSERT-C-term-CFP + hSERT-C-term-YFP) for the carboxyl-terminal halves. These values are significantly different from the reference based on analysis of variance and Scheffé's *post hoc* test ($p < 0.05$). Expression of the amino- and carboxyl-terminal halves together prolonged the lifetime to 23.5 ± 2.3 s ($n = 22$) (CFP-hSERT-N-term + hSERT-C-term-YFP) and to 24.4 ± 2.3 s ($n = 31$) (hSERT-C-term-CFP + YFP-hSERT-N-term). Thus, the amino-terminal half interacts with the carboxyl-terminal half in intracellular membrane compartments; this interaction is not strong enough to reconstitute a functional transporter (Fig. 1, B and C) that is able to overcome intracellular retention.

Based on these data, we conclude that hSERT has to contain

of CFP-hSERT-YFP (upper panel), CFP-hSERT + hSERT-YFP (middle panel), and hSERT-CFP (in the absence of an acceptor fluorophore; lower panel). B, decay of intensity (in regions of interest) was quantified in successive pictures to generate the indicated decay curves; the solid lines were drawn by fitting the data points to an equation describing a monoexponential decay. Data points represent means \pm S.D. from three independent experiments. C, donor photobleaching lifetimes were determined from decay curves similar to those shown in B. The numbers in the bars indicate the number of curves from which the respective average lifetime was calculated. CFP-hSERT-N-term is the internal control (bleaching of CFP in the absence of any acceptor); it has the shortest donor photobleaching lifetime, which is significantly different from all others (+). The double-tagged CFP-hSERT-YFP showed the highest yield of FRET, which is significantly different from all others (~). The combination CFP-hSERT + YFP-hSERT was significantly different from the other combinations of tagged full-length hSERTs (*); the lifetimes of CFP-hSERT-N-term + YFP-hSERT-N-term were significantly different from those of hSERT-C-term-CFP + hSERT-C-term-YFP (#) (all $p < 0.05$; analysis of variance followed by Scheffé's *post hoc* test). D, to measure DRAP, we acquired a donor (CFP) image before and after photobleaching using the YFP setting for 90 s (excitation = 500 nm, dichroic mirror = 525 nm, and emission = 535 nm). DRAP was quantified by FRET efficiency as described under "Experimental Procedures." *rel.*, relative.

more than one domain important for oligomerization, *viz.* at least one each in the amino- and carboxyl-terminal halves of the transporter. Oligomer formation is required for efficient export of transporters from the ER, and point mutations that suppress oligomerization result in intracellular retention (9). Although the half-molecules of hSERT do form oligomers, these are retained in intracellular compartments. This presumably arises from the disruption of ER export signals that are formed by discontinuous segments. Regardless of the underlying basis, the intracellular retention can be exploited as an interaction assay. We therefore coexpressed YFP-tagged full-length hSERT and the CFP-tagged half-molecules. This allows each molecule to be visualized individually, *viz.* the intracellularly retained half-molecule with the CFP filter (Fig. 3, *B* and *D*) and the fate of the full-length transporter with the YFP filter set (Fig. 3, *A* and *B*); in addition, we used limiting amounts of the plasmid driving expression of the half-molecule. This resulted in a mixture of cells that expressed both full-length and severed transporters and exclusively full-length hSERT; the latter cells served as an internal control. In cells that expressed either the amino- or carboxyl-terminal half-molecule and the full-length transporter, hSERT was retained within the cell. In contrast, in cells that expressed only the full-length transporter, hSERT was efficiently inserted into the plasma membrane (YFP filter) (Fig. 3, *A* and *C*).

Obviously, only those transporters that are inserted into the plasma membrane support uptake of substrate. Thus, the retention of hSERT by the half-molecules can also be quantified as the average effect on the uptake of [³H]5-HT by a transiently transfected cell population. HEK293 cells were therefore transfected with a constant amount of plasmid DNA encoding full-length hSERT, increasing amounts of DNA encoding the half-molecules, and empty plasmid to keep the total amount of DNA constant. The uptake of [³H]5-HT was progressively reduced as the expression of the amino-terminal (Fig. 3*E*, *closed circles*) and carboxyl-terminal (*open triangles*) half-molecules was forced by raising the amount of cognate plasmid DNA. We noted that inhibition of [³H]5-HT uptake was observed over a reasonably comparable range of plasmid DNA. However, it is self-evident that quantitative interpretations are limited by the fact that the amount of protein produced per μg of plasmid DNA may vary considerably.

Aggregated fragments may have caused nonspecific retention of the full-length transporter in the ER. This was ruled out by coexpressing the human dopamine D₂ receptor tagged at its carboxyl terminus with CFP (hD2-CFP) and either of the YFP-labeled half-molecules of hSERT in HEK293 cells. Neither the amino-terminal (YFP-hSERT-N-term) (Fig. 3*G*) nor the carboxyl-terminal (hSERT-C-term-YFP) (Fig. 3*I*) half of hSERT caused accumulation of the receptor within the cell (CFP filter) (Fig. 3, *F* and *H*) to an extent that exceeded retention in the absence of half-molecules (data not shown). The extent of retention of hD2-CFP in cells expressing both constructs was also quantified by having a blinded observer score a random selection of transfected cells for intracellular retention: CFP-hD2 + YFP-hSERT-N-term, 16%; and CFP-hD2 + hSERT-C-term-YFP, 10%. This extent of intracellular retention was also observed in cells transfected with the receptor alone.

Discontinuous Nature of the Oligomeric Interface—Taken together, the findings demonstrate that the carboxyl-terminal half of hSERT contributes an interface to oligomer formation. We generated fragments that comprised two neighboring TM segments of hSERT and YFP: YFP-hSERT-TM1/2, -TM3/4, -TM5/6, -TM7/8, and -TM9/10 and hSERT-TM11/12-YFP. Upon expression in HEK293 cells, they were not delivered to the plasma membrane. Hence, it was possible to exploit intracel-

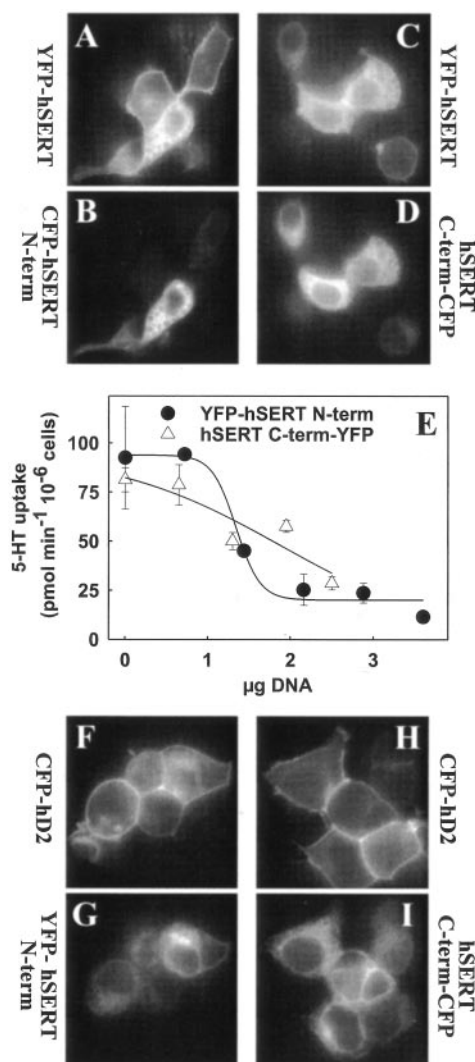


FIG. 3. Intracellular retention of full-length hSERT by the amino- and carboxyl-terminal halves of SERT. HEK293 cells were transiently transfected with plasmids encoding the YFP-labeled full-length transporter constructs (YFP-hSERT (*A* and *C*) and hSERT-YFP (*B* and *D*)) and the CFP-labeled severed transporter constructs (CFP-hSERT-N-term (*A* and *C*) and hSERT-C-term-CFP (*B* and *D*)). For fluorescence microscopy, images were captured with the CFP (*B* and *D*) and YFP (*A* and *C*) filter sets; cells representative of three experiments are shown. For 5-HT uptake (*E*), cells were transfected with 1 μg of plasmid encoding the full-length transporter and increasing amounts of plasmid for the half-transporter (as indicated). The total DNA amount in the transfection was kept constant by adding empty plasmid pKRSFA. The uptake of [³H]5-HT was determined as described in the legend to Fig. 1. HEK293 cells were transiently transfected with plasmids encoding hD2-CFP and YFP-labeled severed transporter constructs (YFP-hSERT-N-term (*F* and *G*) and hSERT-C-term-YFP (*H* and *I*)). Images were captured with the CFP (*F* and *H*) and YFP (*G* and *I*) filter sets; cells representative of three independent experiments are shown.

lular retention of CFP-tagged hSERT by each fragment as an assay to determine which fragment interacted with the full-length transporter. Fig. 4*A* shows the fluorescence micrographs (using YFP and CFP filter sets) of cells expressing individual YFP-tagged fragments and the CFP-tagged full-length transporter. When expressed in the same cell, constructs comprising TM1/2, TM5/6, and TM11/12 prevented full-length hSERT from being correctly inserted into the plasma membrane. In contrast, the other fragments (TM3/4, TM7/8, and TM9/10) failed to retain the full-length transporter. The extent of retention in cells expressing both constructs was also quantified by having an unbiased observer score a random selection of trans-

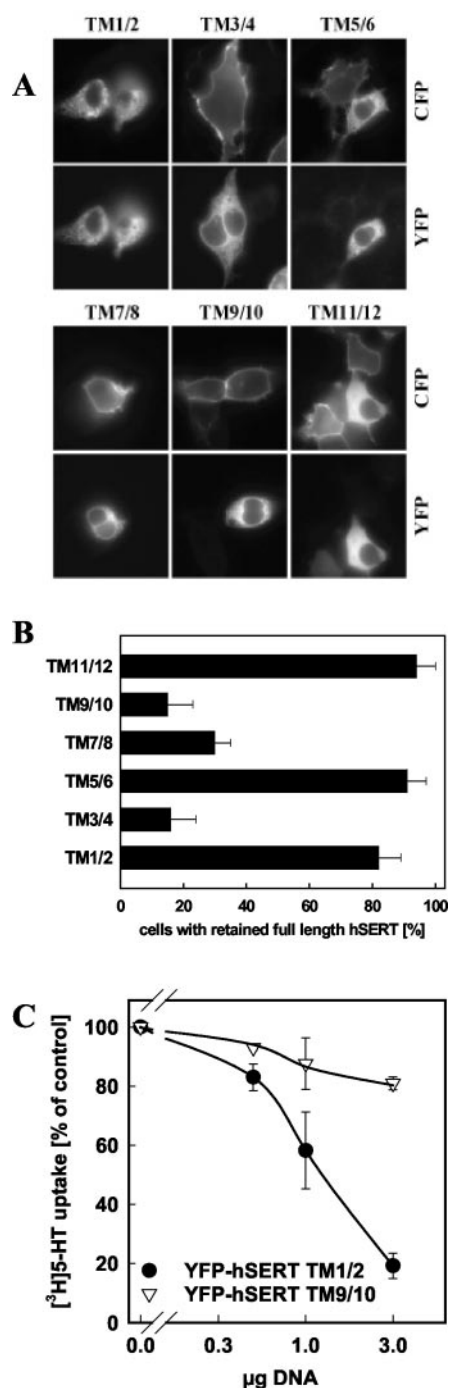


FIG. 4. Intracellular retention of CFP-hSERT through fragments comprising two adjacent TM helices. HEK293 cells were transfected with plasmids encoding CFP-hSERT and YFP-labeled constructs of neighboring TMs as indicated. *A*, images were captured with the CFP and YFP filter sets. *B*, shown is the extent of retention of full-length CFP-hSERT in cells expressing both constructs (quantification by an unbiased observer); data are means \pm S.D. from three independent experiments. *C*, shown is 5-HT uptake. Cells were transfected with 1 μ g of plasmid encoding the full-length transporter and increasing amounts of plasmid encoding the YFP-labeled constructs of neighboring TMs as indicated. The total DNA amount in the transfection was kept constant by adding empty plasmid pKSPA. The uptake of [³H]5-HT was determined as described in the legend to Fig. 1 and normalized to uptake observed in the absence of cotransfected fragments to account for variation in absolute expression levels between individual experiments.

fectected cells for intracellular retention (Fig. 4*B*). The observer was blinded with respect to the transfection protocol in at least three independent transfections. This quantification gave the

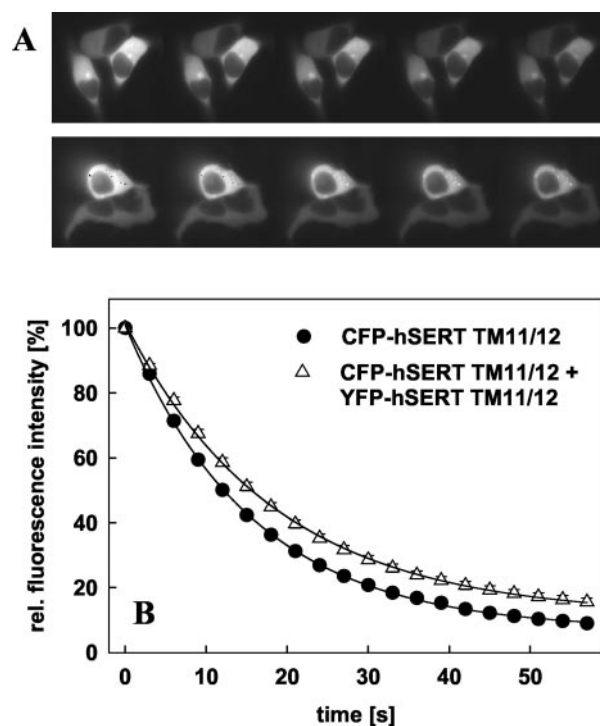


FIG. 5. Donor photobleaching FRET microscopy with fragments comprising two adjacent TM helices. The indicated combinations were coexpressed in HEK293 cells; donor photobleaching FRET was measured as described in the legend to Fig. 2. *A*, representative images (3-s intervals) illustrate the decrease in the donor fluorescence of CFP-hSERT-TM11/12 (in the absence of an acceptor fluorophore; upper panel) and CFP-hSERT-TM11/12 + YFP-hSERT-TM11/12 (lower panel). *B*, the decay of intensity (in regions of interest) was quantified as described in the legend to Fig. 2*B*. *rel.*, relative.

following estimates for the proportion of cells in which the full-length transport was retained within the cell by the fragment: 82 \pm 7% (TM1/2), 16 \pm 8% (TM3/4), 91 \pm 6% (TM5/6), 30 \pm 5% (TM7/8), 15 \pm 8% (TM9/10), and 94 \pm 6% (TM11/12). Alternatively, intracellular retention of hSERT by the fragments was also assessed by measuring the decline in cellular 5-[³H]HT uptake that resulted from the loss of surface expression. This approach gave similar results, which are shown for TM1/2 and TM9/10 in Fig. 4*C*.

These observations suggest that there are at least three contact sites. To determine whether they support homophilic or heterophilic interactions, we performed donor photobleaching FRET with these different combinations of six fragments tagged with CFP or YFP (as indicated in Fig. 6). This ought to allow detection of the interaction partners of the candidate oligomerization domains in the oligomer. The decay of fluorescence was substantially slower in the coexpressed pair CFP-hSERT-TM11/12 + YFP-hSERT-TM11/12 than in CFP-hSERT-TM11/12 (Fig. 5, *A* and *B*). The results of donor photobleaching measurements are summarized for CFP-hSERT-TM1/2 and hSERT-TM11/12-CFP in Fig. 6*A*: bleaching of CFP-hSERT-TM1/2 was only significantly ($p < 0.001$) delayed by YFP-tagged TM1/2 compared with sole expression of CFP-hSERT. In contrast, neither YFP-tagged TM5/6 and TM11/12 (Fig. 6*A*) nor the other YFP-tagged fragments (data not shown) protected CFP-hSERT-TM1/2 against bleaching. Similarly, coexpression of only hSERT-TM11/12-CFP and hSERT-TM11/12-YFP resulted in a significant ($p < 0.001$) increase in the lifetime of fluorescence decay (Fig. 6*A*). With all other tested combinations, the increase was not significant. As depicted in Fig. 6*B*, we failed to find any evidence for resonance energy

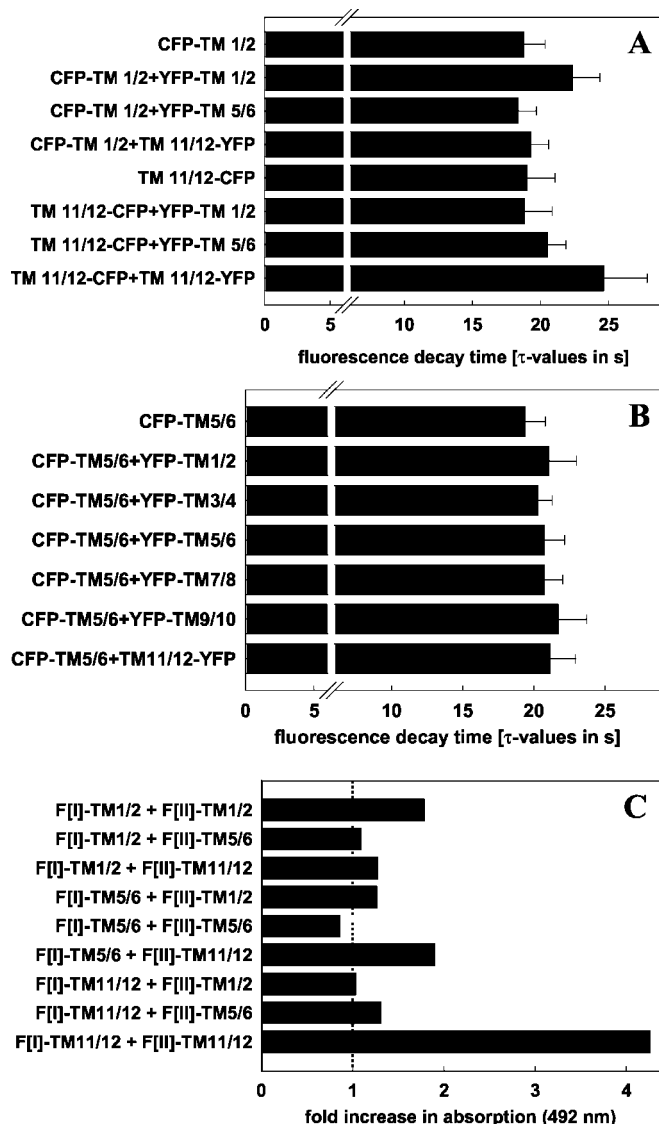


FIG. 6. Donor photobleaching decay lifetimes obtained (A and B) and β -lactamase protein fragment complementation assay performed (C) with combinations of fragments comprising two adjacent TM helices. Shown are the donor photobleaching decay lifetimes of constructs CFP-hSERT-TM1/2 and hSERT-TM11/12-CFP (A) and CFP-hSERT-TM5/6 (B) as donors coexpressed with the indicated acceptors. Decay lifetimes were determined as described in the legend to Fig. 2 ($n = 20-50$); the combinations CFP-hSERT-TM1/2 + YFP-hSERT-TM1/2 and hSERT-TM11/12-CFP + hSERT-TM11/12-YFP are significantly different from their respective controls (CFP alone) and all other combinations at $p < 0.001$ (analysis of variance and Scheffé's *post hoc* test). Shown are the results from the β -lactamase protein fragment complementation assay (C). HEK293 cells were co-transfected with plasmids encoding the indicated combinations of constructs comprising two adjacent TM helices of hSERT fused to either fragment of the enzyme (F[I] and F[II]). Interaction between coexpressed constructs was measured by determining enzymatic activity in membrane preparations (20 mg/sample). Cleavage of the substrate nitrocefin (resulting in a color change from yellow to red) was measured at 492 nm. Under basal conditions (transfection with only one fragment), the absorbance measured at 492 nm was $\sim 0.06-0.08$; the maximum absorbance obtained with the combination F[I]-TM11/12 + F[II]-TM11/12 was 0.4. Values shown are -fold increases in absorbance in comparison with transfection with the corresponding F[I] fragment alone. Data are from one representative experiment done in triplicate and reproduced twice.

transfer with CFP-hSERT-TM5/6 regardless of which possible acceptor was employed.

As an independent method, we also used the β -lactamase protein fragment complementation assay. The enzyme is bi-

sected into two lobes that fail to interact with each other. Enzymatic activity is restored if the lobes are brought into close vicinity. We generated constructs of two neighboring TMs (TM1/2, TM5/6, and TM11/12) fused to either half of the enzyme (F[I] and F[II]). Interaction was verified by enzymatic turnover of nitrocefin, a substrate of β -lactamase that yields a red cleavage product (Fig. 6C). Modest increases were detected upon coexpression of F[I]-TM1/2 and F[II]-TM1/2 (1.8-fold) and of F[I]-TM5/6 and F[II]-TM11/12 (1.9-fold). In contrast, a robust increase was seen with F[I]-TM11/12 and F[II]-TM11/12 (4.3-fold).

DISCUSSION

Several contact sites have been mapped that support the oligomerization in Na^+/Cl^- -dependent neurotransmitter transporters; these include a leucine heptad repeat in TM2 (7, 12) and a glycoprotein A-like motif in TM6 (6). In addition, the TM4 segments have recently been shown to form a symmetrical dimeric interface in the human dopamine transporter (24). These interaction sites are all confined to the amino-terminal half of the protein. The present experiments identified a new contact site in the carboxyl-terminal half of the hydrophobic core, *viz.* within TM11 and TM12. This conclusion is based on the following findings. (i) The carboxyl-terminal half of hSERT (*i.e.* the last six TM segments) was capable of self-association; it also retained the full-length transporter within the cell. (ii) A fragment that comprised only TM11 and TM12 also retained the full-length transporter within the cell. (iii) This TM11/12 fragment also displayed a strong ability to self-associate, as assessed by two independent approaches, *viz.* FRET microscopy and β -lactamase complementation assay. The primary amino acid sequence does not reveal any obvious motif other than the presence of many serine residues. These may support association of TM helices (25). However, appropriate point mutations (alanine substitutions) have been disappointing.³

We also detected a homophilic interaction with the fragment comprising TM1 and TM2. Our earlier work (12) identified a leucine heptad repeat in TM2 of γ -aminobutyric acid transporter-1 that is important for oligomer formation. It is tempting to draw an analogy with transcription factors (26) and with the membrane protein phospholamban (27) and to postulate that the leucine heptad repeats in TM2 pair to form leucine zippers. Leucine heptad repeats can form leucine zippers when introduced into artificial hydrophobic TM segments, and a leucine zipper does support pentamer formation in phospholamban (28). However, TM2 of SERT does not contain a perfect leucine heptad repeat because Ala¹²⁵ is present instead of leucine in the second repeat. In addition, there are many arguments that have been raised against a widespread role of leucine zippers in driving the association in TM proteins (26). Finally, all neurotransmitter transporters contain a conserved glycine residue (Gly¹²⁹ in hSERT) in the fourth position of the second repeat, *i.e.* sandwiched between the second and third leucines, which are one helical turn above and below this glycine. In SERT, however, alanine substitutes for the second leucine. It is difficult to envision how this large cavity can be filled to form a stable leucine zipper. Thus, the structure that supports a homophilic interaction in TM1/2 remains to be determined.

We ruled out that, in our experiments, nonspecific aggregation of proteins in the ER resulted in nonspecific FRET. Of all the fragment combinations that were tested, only TM1/2 and TM11/12 displayed significant FRET when tested for homophilic interaction. In fact, we failed to detect FRET with TM5/6. This is somewhat surprising because the glycoprotein A-like motif (consensus sequence GVXXGVXXA) is also present

³ V. M. Korkhov and M. Freissmuth, unpublished data.

in TM6 of SERT, with the corresponding stretch of amino acids being GPGFGVLLA. A substitution of valine with proline in the second position can still support strong membrane helix-helix interaction (29). Given the strong degree of homology between monoamine transporters, it is reasonable to assume that TM6 also supports a homophilic interaction in SERT. Nevertheless, with the isolated fragment TM5/6, we failed to detect a direct interaction with itself or with any other fragment by FRET microscopy. This may possibly reflect an incorrectly folded structure in the TM5/6 fragment. Similarly, the β -lactamase protein fragment complementation assay did not detect any homophilic interaction of TM5/6, but it revealed a modest degree of interaction between TM5/6 and TM11/12. However, heterophilic contacts that are detected with small fragments are difficult to interpret, for they may reflect intramolecular contacts between helices rather than intermolecular contacts. This caveat also applies to our third assay, *viz.* the retention assay. This assay relies on the fact that oligomerization of many Na^+/Cl^- -dependent neurotransmitter transporters is a prerequisite for ER export (reviewed in Ref. 9). Thus, disruption of the oligomer by competing for intermolecular contacts results in retention. However, it is obvious that a TM segment that can efficiently compete for intramolecular contacts can also cause intracellular retention because it interferes with folding of the monomeric unit.

The presence of two homophilic contact sites precludes a dimeric structure; this constraint has been pointed out some 20 years ago based on a logical argument (13). The most plausible arrangement is a tetramer composed of two dimeric units: one homophilic interaction domain tethers together two molecules, and the second interaction domain forms the tetrameric structure. This arrangement has also been recently proposed for the dopamine transporter (24). However, this arrangement does not result in a self-contained structure. In other words, in this model, transporters are prone to form a larger array-like structure in the membrane. There is evidence for an array-like structure of the Na^+/H^+ antiporter NhaA (30, 31). Many membrane proteins have 12 TM helices, and this is particularly true for neurotransmitter transporters (32). Obviously, it is difficult to resist the temptation to implicitly assume that the same or a related topology holds true for most transporters. Recently, the crystal structures of several bacterial transporters, *viz.* lactose permease (10), the glycerol 3-phosphate transporter (11) and the multidrug efflux transporter AcrB (33), have been resolved. These transporters all share a point symmetry within the monomer, with TM1 opposite of TM7, TM2 opposite of TM8, and TM6 opposite of TM12. However, AcrB is a trimer, whereas lactose permease and the glycerol 3-phosphate transporter are monomers. In addition, the symmetrical arrangement of helices requires a long intracellular loop between TM6 and TM7,

which is not present in hSERT. Thus, any extrapolation must be exercised with caution.

Acknowledgments—We thank Dr. Stephen W. Michnick (Département de Biochimie, Université de Montréal, Montréal, Canada) for providing the plasmids for the β -lactamase protein fragment complementation assay and Marion Holy for invaluable technical assistance with cell cultures.

REFERENCES

- Scholze, P., Zwach, J., Kattinger, A., Pifl, C., Singer, E. A., and Sitte, H. H. (2000) *J. Pharmacol. Exp. Ther.* **293**, 870–878
- Schmid, J. A., Scholze, P., Kudlacek, O., Freissmuth, M., Singer, E. A., and Sitte, H. H. (2001) *J. Biol. Chem.* **276**, 3805–3810
- Sorkina, T., Doolen, S., Galperin, E., Zahniser, N. R., and Sorkin, A. (2003) *J. Biol. Chem.* **278**, 28274–28283
- Eskandari, S., Kreman, M., Kavanaugh, M. P., Wright, E. M., and Zampighi, G. A. (2000) *Proc. Natl. Acad. Sci. U. S. A.* **97**, 8641–8646
- Kilic, F., and Rudnick, G. (2000) *Proc. Natl. Acad. Sci. U. S. A.* **97**, 3106–3111
- Hastrup, H., Karlin, A., and Javitch, J. A. (2001) *Proc. Natl. Acad. Sci. U. S. A.* **98**, 10055–10060
- Torres, G. E., Carneiro, A., Seamans, K., Fiorentini, C., Sweeney, A., Yao, W. D., and Caron, M. G. (2003) *J. Biol. Chem.* **278**, 2731–2739
- Kocabas, A. M., Rudnick, G., and Kilic, F. (2003) *J. Neurochem.* **85**, 1513–1520
- Sitte, H. H., and Freissmuth, M. (2003) *Eur. J. Pharmacol.* **479**, 229–236
- Abramson, J., Smirnova, I., Kasho, V., Verner, G., Kaback, H. R., and Iwata, S. (2003) *Science* **301**, 610–615
- Huang, Y., Lemieux, M. J., Song, J., Auer, M., and Wang D. N. (2003) *Science* **301**, 616–620
- Scholze, P., Freissmuth, M., and Sitte, H. H. (2002) *J. Biol. Chem.* **277**, 43682–43690
- Klingenberg, M. (1981) *Nature* **290**, 449–454
- Miyawaki, A., and Tsien, R. Y. (2000) *Methods Enzymol.* **327**, 472–500
- Galarneau, A., Primeau, M., Trudeau, L. E., and Michnick, S. W. (2002) *Nat. Biotechnol.* **20**, 619–622
- Jess, U., El Far, O., Kirsch, J., and Betz, H. (2002) *Biochem. Biophys. Res. Commun.* **294**, 272–279
- Beckman, M. L., Bernstein, E. M., and Quick, M. W. (1998) *J. Neurosci.* **18**, 6103–6112
- Deken, S. L., Beckman, M. L., Boos, L., and Quick, M. W. (2000) *Nat. Neurosci.* **3**, 998–1003
- Perego, C., Bulbarelli, A., Longhi, R., Caimi, M., Villa, A., Caplan, M. J., and Pietrini, G. (1997) *J. Biol. Chem.* **272**, 6584–6592
- Torres, G. E., Yao, W. D., Mohn, A. R., Quan, H., Kim, K. M., Levey, A. I., Staudinger, J., and Caron, M. G. (2001) *Neuron* **30**, 121–134
- Sung, U., Apparsundaram, S., Galli, A., Kahlig, K. M., Savchenko, V., Schroeter, S., Quick, M. W., and Blakely, R. D. (2003) *J. Neurosci.* **23**, 1697–1709
- Förster, T. (1948) *Ann. Physik.* **2**, 55–75
- Schmid, J. A., and Sitte, H. H. (2003) *Curr. Opin. Oncol.* **15**, 55–64
- Hastrup, H., Sen, N., and Javitch, J. A. (2003) *J. Biol. Chem.* **278**, 45045–45048
- Dawson, J. P., Weinger, J. S., and Engelman, D. M. (2002) *J. Mol. Biol.* **316**, 799–805
- Zhou, F. X., Cocco, M. J., Russ, W. P., Brunger, A. T., and Engelman, D. M. (2000) *Nat. Struct. Biol.* **7**, 154–160
- Cornea, R. L., Autry, J. M., Chen, Z., and Jones, L. R. (2000) *J. Biol. Chem.* **275**, 41487–41494
- Li, H., Cocco, M. J., Steitz, T. A., and Engelman, D. M. (2001) *Biochemistry* **40**, 6636–6645
- Russ, W. P., and Engelman, D. M. (2000) *J. Mol. Biol.* **296**, 911–919
- Williams, K. A. (2000) *Nature* **403**, 112–115
- Gerchman, Y., Rimon, A., Venturi, M., and Padan, E. (2001) *Biochemistry* **40**, 3403–3412
- Busch, W., and Saier, M. H., Jr. (2002) *Crit. Rev. Biochem. Mol. Biol.* **37**, 287–337
- Murakami, S., Nakashima, R., Yamashita, E., and Yamaguchi, A. (2002) *Nature* **419**, 587–593